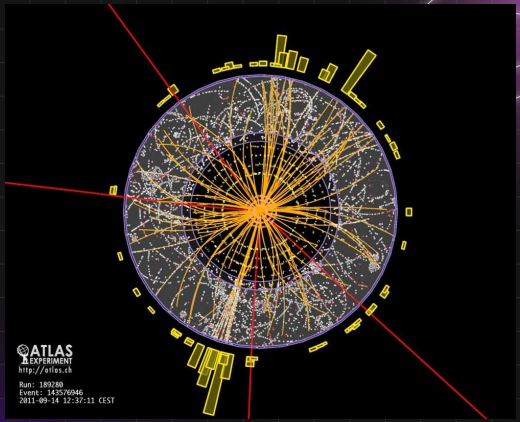


# Higgs Physics

Anirudhya, Hamsini, Sheersh

IISc Bengaluru, April 11, 2025

# Outline

# Introduction

- The Higgs mechanism is the process by which gauge bosons (like the W and Z bosons in the Standard Model) acquire mass without violating gauge invariance
- Glashow-Weinberg–Salam model provides a unified description of the electromagnetic and weak interactions through a gauge theory based on the symmetry group $SU(2) \times U(1)$.
- This unification successfully explains phenomena such as weak interactions, neutral currents, and spontaneous symmetry breaking, laying the foundation for electroweak theory

# The Problem Without the Higgs Mechanism

- In gauge theories, like QED and the Electroweak Theory, gauge bosons must remain massless to preserve gauge invariance and renormalizability. A naive mass terms brings issues:
  - **Gauge Invariance Violation:** A mass term explicitly breaks gauge symmetry, which is essential for renormalizability.
  - **Loss of Renormalizability:** Longitudinal polarizations of massive gauge bosons cause bad high-energy behavior, making amplitudes like $W^+W^- \to W^+W^-$ grow as $E^2$, violating unitarity.
  - **Fermion Mass Problem:** Explicit mass terms break chiral gauge symmetry, leading to non-renormalizable interactions.

# The Problem Without the Higgs Mechanism

- Further Consequences
  - Weak boson scattering amplitudes become uncontrollable at high energies - unitarity violation.
  - Keeping the photon massless while giving mass to $W$ and $Z$ requires an alternative mechanism.
  - Experimental data on particle masses and interactions would not match theoretical predictions.
- The Higgs mechanism provides a natural, gauge-invariant, and renormalizable way to give mass to gauge bosons and fermions, restoring consistency to the electroweak theory.

# Why Do Particles Have Mass?

- The Higgs field permeates space, providing mass to fundamental particles.
- Without the Higgs mechanism, electrons and quarks would be massless, preventing atom formation.
- Weak bosons (W, Z) acquire mass via spontaneous breaking of $SU(2)_L \times U(1)_Y$.
- Fermions (quarks, leptons) gain mass through Yukawa interactions with the Higgs field
- **Photon:** Remains massless as $U(1)_{EM}$ is unbroken.
- **Gluons:** Remain massless because QCD's $SU(3)_C$ symmetry remains unbroken.

# Introduction to Symmetry Breaking

- Symmetry breaking: A symmetric system transitions into an asymmetric state.
- Types of Symmetry Breaking
  - **Explicit Symmetry Breaking:** An external influence disrupts symmetry.
  - **Spontaneous Symmetry Breaking (SSB):** Laws remain symmetric, but the system selects a non-symmetric state.
  - **Dynamical Symmetry Breaking (DSB):** Quantum interactions dynamically induce symmetry breaking through VEVs.

# Spontaneous Symmetry Breaking

- SSB occurs when the equations of a system remain symmetric, but the lowest-energy state (vacuum state) does not exhibit that symmetry.
- SSB can occur in Global Symmetry and Local (Gauge) Symmetry.
- In gauge theories, it leads to mass generation (Higgs mechanism).

# Goldstone Bosons

- Goldstone's theorem states that when a continuous global symmetry is spontaneously broken, the spectrum will contain massless scalar bosons (Goldstone bosons).
- When the symmetry is gauged, Goldstone's theorem fails.
- In the gauged case, the Goldstone bosons are absorbed by the gauge fields, which leads to the gauge bosons acquiring mass (Higgs mechanism).

- The number of broken generators equals the number of massless Goldstone bosons.
- Mathematically, if a set of scalar fields $\phi^a$ transforms under a symmetry group such that the potential $V(\phi)$ acquires a nonzero vacuum expectation value $\langle\phi\rangle$, then the associated Noether currents $J^{\mu a}$ satisfy:

$$\partial_\mu J^{\mu a} = 0,$$

  where each broken generator corresponds to a massless Goldstone boson.
- But when spontaneously broken symmetry couple to gauge fields, the Goldstone bosons become the longitudinal polarization modes of massive gauge bosons.

# Longitudinal Degrees of Freedom

- A massless spin-1 particle: two transverse polarization states.
- A massive spin-1 particle: additional longitudinal polarization state.
- The Higgs mechanism provides this extra degree of freedom by turning a Goldstone boson into the longitudinal mode of the gauge boson.
- Gauge Coupling Behavior:
  - When gauge coupling $(g) \to 0$, the gauge bosons become massless, and the Goldstone bosons reappear as physical degrees of freedom.
  - When $g \neq 0$, the longitudinal mode is absorbed, and the gauge bosons acquire mass.

# Spontaneous Symmetry Breaking in a Scalar Field Theory

- Consider a complex scalar field $\phi$ with the Lagrangian:

$$L = \partial_\mu \phi^\dagger \partial^\mu \phi - V(\phi) \tag{1}$$

$$\text{Where, } V(\phi) = -\mu^2 |\phi|^2 + \lambda |\phi|^4. \tag{2}$$

.

- For stability, $\lambda > 0$, and the term $-\mu^2$ makes the mass term tachyonic, leading to spontaneous symmetry breaking.
- Minimizing $V$ gives $\phi^\dagger \phi = \frac{\mu^2}{2\lambda}$.
- Then vacuum solution : $\langle \phi \rangle = \frac{v}{\sqrt{2}}, \quad v = \frac{\mu}{\sqrt{\lambda}}$.
- Since the Lagrangian is invariant under global U(1) symmetry, but the vacuum is not, one degree of freedom becomes a massless Goldstone boson.

# Spontaneous Symmetry Breaking in Local Gauge theory

- Consider a local gauge theory with a gauge field $A_\mu$ coupled to the complex scalar field:

$$L = |D_\mu \phi|^2 - V(\phi), \tag{3}$$

- Expanding around the vacuum: $\phi = \frac{1}{\sqrt{2}}(v + h(x))e^{i\theta(x)/v}$. Here, $h(x)$ is a real scalar field, and $\theta(x)$ is the Goldstone mode
- Substituting into the Lagrangian:

$$L = \frac{1}{2}(\partial_\mu h)^2 + \frac{1}{2}g^2 v^2 A_\mu A^\mu - V(h). \tag{4}$$

- $V(\phi)$ induces SSB, gives gauge boson a mass!:

$$M_A^2 = g^2 |\langle \phi \rangle|^2. \tag{5}$$

# Higgs Mechanism in Electroweak Theory

- When the Higgs mechanism breaks the electroweak symmetry $SU(2)_L \times U(1)_Y$ down to $U(1)_{\text{EM}}$, the gauge bosons acquire masses.
- Higgs doublet acquires a vacuum expectation value (VEV)
- The Higgs kinetic term: $\mathcal{L} = |D_\mu H|^2$
- The covariant derivative of the Higgs field contains interactions with the $SU(2)_L$ and $U(1)_Y$ gauge fields:

$$D_\mu H = \left( \partial_\mu - i\frac{g}{2} W_\mu^a \tau^a - i\frac{g'}{2} B_\mu \right) H.$$

(Give mass terms for the gauge bosons after the Higgs acquires a vev.)

- Define charged $W$ bosons, $W^{\pm} = \frac{1}{\sqrt{2}}(W^1 \mp iW^2)$, the mass is given by:$M_W = \frac{1}{2}gv$.
- The neutral gauge bosons $W^3_\mu$ (from $SU(2)_L$) and $B_\mu$ (from $U(1)_Y$) mix[1] to form the physical $Z$ boson and the photon $\gamma$. This mixing is described by the Weinberg angle $\theta_W$:

$$Z_\mu = \cos\theta_W W^3_\mu - \sin\theta_W B_\mu,$$
$$A_\mu = \sin\theta_W W^3_\mu + \cos\theta_W B_\mu.$$

Here, Weinberg angle is defined as:

$$\tan\theta_W = \frac{g'}{g}.$$

The mass of the $Z$ boson is:

$$M_Z = \frac{1}{2}\sqrt{g^2 + g'^2}v.$$

The photon $A_\mu$ remains massless because electromagnetism $U(1)_{\text{EM}}$ is unbroken.

[1] PW Higgs, Phys. Rev. Lett. 19, 21 (1967)

# Prediction of Neutral Currents

- The Weinberg–Salam model predicts the existence of *neutral current interactions*, mediated by the *Z boson*.
- The interaction of the Z boson with a fermion (f) is given by the Lagrangian:

$$\mathcal{L}_{\text{NC}} = \frac{g}{\cos\theta_W} \bar{f} \gamma^\mu (g_V - g_A \gamma^5) f Z_\mu \tag{6}$$

- The vector and axial-vector couplings are given by:

$$g_V = T^3 - 2Q \sin^2\theta_W, \quad g_A = T^3 \tag{7}$$

- The electroweak theory predicted that neutrinos should interact without changing flavor via the neutral current interaction.
- These interactions were experimentally verified in neutrino scattering experiments at CERN in 1973, providing strong support for the model.

# Higgs Couplings to Fermions

- Fermions gain mass through Yukawa interactions:

$$\mathcal{L}_Y = -y_f \bar{\psi}_L \Phi \psi_R + \text{h.c.} \tag{8}$$

- When $\Phi$ acquires a vacuum expectation value (VEV):

$$M_f = \frac{y_f v}{\sqrt{2}}. \tag{9}$$

- The mass of a fermion depends on its Yukawa coupling to the Higgs field. If $y_f$ is large, the fermion mass will also be large.

# Higgs Potential

- The potential $V(\phi_1^2 + \phi_2^2)$ has a Mexican hat shape, with minima at a nonzero field value $\phi_0$.
- The Higgs potential is given by:

$$V(\Phi) = \mu^2 \Phi^\dagger \Phi + \lambda (\Phi^\dagger \Phi)^2. \tag{10}$$

- Expressing the Higgs doublet in terms of real component fields:

$$\Phi = \frac{1}{\sqrt{2}}(\phi_1 + i\phi_2), \tag{11}$$

we expand the potential as:

$$V(\phi_1, \phi_2) = \frac{\mu^2}{2}(\phi_1^2 + \phi_2^2) + \frac{\lambda}{4}(\phi_1^2 + \phi_2^2)^2. \tag{12}$$

- For $\mu^2 > 0$, the minimum is at $\phi_1 = \phi_2 = 0$.
- For $\mu^2 < 0$, the vacuum expectation value (VEV) is given by:

$$\phi_1^2 + \phi_2^2 = \frac{\mu^2}{\lambda}. \tag{13}$$

leads to spontaneous symmetry breaking (SSB). This creates a "Mexican hat" potential with a circle of minima at $|\phi| = v$, leading to an infinite set of possible vacuum states.

Key Consequences:

- **SSB**: The system selects a vacuum state, breaking the symmetry.
- **Higgs Mechanism**: The Higgs boson corresponds to radial oscillations, while Goldstone bosons (massless modes) are absorbed by $W^{\pm}$ and $Z$ bosons, giving them mass.
- **Electroweak Mass Generation**: Explains why weak bosons have mass while the photon remains massless.

# Oscillations in the Higgs Potential

After symmetry breaking, two types of oscillations occur:

- **Radial (Higgs mode)**: Fluctuations in the Higgs boson mass, with mass given by $m_h^2 = 2\lambda v^2$.
- **Angular (Goldstone mode)**: Corresponds to massless modes, which are "eaten" by gauge bosons, making them massive.

Damped oscillations occur due to Higgs boson decay into Standard Model particles, such as $h \to 2Z, 2W, b\bar{b}, gg, \gamma\gamma$. In cosmology, Higgs oscillations could impact early universe dynamics, including reheating after inflation.

- **Equations of Motion for Fluctuations[2]:**
  We are given a system with small oscillations $\Delta\phi_1, \Delta\phi_2, A_\mu$ around the vacuum. These correspond to the fluctuations of the scalar field and the gauge field after spontaneous symmetry breaking (SSB). The equations governing these fluctuations are:

$$\begin{aligned} \partial_\mu \left(\partial^\mu(\Delta\phi_1) - e\phi_0 A^\mu\right) &= 0, \\ \left(\partial^2 - 4\phi_0^2 V''(\phi_0^2)\right) \Delta\phi_2 &= 0, \\ \partial^\nu F_{\mu\nu} &= e\phi_0 \left(\partial_\mu(\Delta\phi_1) - e\phi_0 A_\mu\right). \end{aligned} \tag{14}$$

  The derived equations indicate:
  - One massive scalar field ($\Delta\phi_2$) with $m_{\phi_2}^2 = (2\phi_0)^2 V''(\phi_0^2)$.
  - The Goldstone boson disappears, giving mass to $A_\mu$ via the Higgs mechanism.
  - The gauge boson acquires mass $m_A = e\phi_0$.
  - If $e = 0$, both the gauge and Goldstone bosons remain massless.
  - Mass generation is directly tied to gauge interactions.

[2] PW Higgs, Phys. Rev. Lett. 13, 6 (1964)

# Spontaneous Symmetry Breaking in Non-Abelian Theories

- When symmetry breaking occurs in a semisimple gauge group, different irreducible representations for scalars lead to various mass generation mechanisms. Gauge fields always belong to the adjoint representation of the symmetry group.
- SU(3) Example: Scalars in the Octet Representation
  - In SU(3), if a scalar octet develops VEVs, only two components (with $Y = 0, I_3 = 0$) remain unabsorbed.
  - Six gauge bosons acquire mass through mixing with the remaining scalar components via the Higgs mechanism.
- Vector Boson Masses
  - The mass spectrum includes:
    - Two vector doublets ($I = 1/2$), with mass splitting due to electromagnetic interactions.
    - An $I = 1$ triplet, whose masses arise from electromagnetic effects.In the absence of electromagnetism, these gauge bosons would be massless.

- Residual Unbroken Symmetry
  - Two massless gauge bosons remain, corresponding to an unbroken Abelian subgroup of SU(3).
  - These correspond to a photon-like field and another massless boson.
- Implications for Electroweak Symmetry Breaking
  - A further mechanism (e.g., weak interactions) breaks hypercharge conservation, giving mass to one remaining gauge boson.
  - The photon remains massless, as expected in the Standard Model.

- Incomplete Multiplets
  - After symmetry breaking, some gauge bosons and scalars become massive while others remain massless.
  - This leads to incomplete multiplets, deviating from the original full symmetry representation.This means that the symmetry-breaking pattern does not preserve full multiplets
- Generalization to Composite Higgs Models
  - If symmetry-breaking scalar fields are not fundamental but arise from bilinear combinations of fermions (e.g., $\Phi \sim \bar{\psi}\psi$), the same symmetry-breaking patterns still occur.
  - This suggests possible dynamical origins for mass generation in strongly coupled gauge theories (e.g., Technicolor models).

# Mass Constraint on Higgs Mass

The Standard Model (SM) Higgs sector allows various possibilities, including an elementary Higgs doublet, multiple Higgs fields (as in supersymmetry), or dynamical symmetry breaking without fundamental scalars. The discovery of a 125 GeV Higgs boson supports the SM but does not rule out alternatives[3].

## Higgs Mass in the SM

After spontaneous symmetry breaking (SSB), one physical Higgs boson remains, with mass given by:

$$M_H = \sqrt{2\lambda v^2} \tag{15}$$

where $\lambda$ is the quartic coupling, and $v = 246$ GeV.
Higgs couplings to other particles are proportional to their masses: $\frac{M}{v}, \frac{M^2}{v}, \left(\frac{M}{v}\right)^2$.
while gauge boson couplings behave as:

$$g^2 v \sim \frac{M^2}{v}. \tag{16}$$

[3] Langacker, The Standard Model and Beyond, 2017

## Theoretical Constraints

The quartic coupling $\lambda$ satisfies vacuum stability:

$$\lambda > 0. \tag{17}$$

Relating $M_H$ to electroweak parameters:

$$M_H^2 = 2\lambda v^2, \quad \lambda = \frac{g^2 M_H^2}{8 M_W^2} = \frac{G_F M_H^2}{\sqrt{2}}. \tag{18}$$

where $G_F \approx 1.2 \times 10^{-5}$ GeV$^{-2}$.

## Renormalization Group Constraints

The running of gauge couplings follows:

$$b_{g_s} = \frac{1}{16\pi^2}\left(11 - \frac{4F}{3}\right) \to -\frac{1}{16\pi^2}(7) \tag{19}$$

$$b_g = \frac{1}{16\pi^2}\left(\frac{22}{3} - \frac{4F}{3} - \frac{n_H}{6}\right) \to -\frac{1}{16\pi^2}\left(\frac{19}{6}\right) \tag{20}$$

$$b_{g'} = \frac{1}{16\pi^2}\left(\frac{20F}{9} + \frac{n_H}{6}\right) \to +\frac{1}{16\pi^2}\left(\frac{41}{6}\right) \tag{21}$$

The running of $\lambda(Q^2)$ and top Yukawa coupling $h_t$ is:

$$\frac{d\lambda(Q^2)}{d\ln Q^2} = \frac{1}{32\pi^2}\left(24\lambda^2 + 24h_t^2\lambda - 24h_t^4 - 3\lambda(3g^2 + g'^2) + \frac{3}{8}\left(2g^4 + (g^2 + g'^2)^2\right)\right), \tag{22}$$

$$\frac{dh_t(Q^2)}{d\ln Q^2} = \frac{1}{32\pi^2}\left(9h_t^3 - h_t\left(8g_s^2 + \frac{9}{4}g^2 + \frac{17}{12}g'^2\right)\right). \tag{23}$$

The couplings on the right-hand side (RHS) are the running couplings at $Q^2$.
The running of $h_t$ is mainly due to vertex corrections, the top quark, and Higgs self-energy diagrams.

# Triviality Bound on $M_H$

- For large $M_H$, the quartic coupling runs as:

$$\lambda(Q^2) = \frac{\lambda(\mu^2)}{1 - \frac{3\lambda(\mu^2)}{4\pi^2} \ln(Q^2/v^2)}. \tag{24}$$

It diverges at the Landau pole $Q_{LP} = ve^{\frac{2\pi^2}{3\lambda(\mu^2)}}$. Requiring $Q_{LP}$ above new physics scale $\Lambda$, the triviality bound is: $M_H < \sqrt{\frac{2\sqrt{2}\pi^2}{3G_F \ln(\Lambda/v)}}$. For different $\Lambda$:

- $\Lambda \sim M_P \Rightarrow M_H \lesssim 140$ GeV.
- $\Lambda \sim 1500$ GeV $\Rightarrow M_H \lesssim 650$ GeV.

Lattice calculations suggest an absolute upper bound of 650–700 GeV.

# Vacuum Stability and Lower Bound on $M_H$

- For small $\lambda$, the running equation simplifies to:

$$\lambda(Q^2) \approx \lambda(v^2) - \frac{3h_t^4}{4\pi^2} \ln \frac{Q^2}{v^2}. \tag{25}$$

Requiring $\lambda(Q^2) > 0$ at $Q = \Lambda$ leads to:

$$M_H^2 = \frac{3h_t^4 v^2}{2\pi^2 G_F} \ln \frac{Q}{v}. \tag{26}$$

For $\Lambda = 1500$ GeV, $M_H \approx 85$ GeV.
For large $\Lambda$, corrections refine the bound:

$$130 \leq M_H \leq 180 \text{ GeV} \quad \text{for } \Lambda = M_P. \tag{27}$$

In the MSSM, where $\lambda$ is not independent, the Higgs mass is limited to: $M_H \lesssim 135$ GeV (or 150 GeV in singlet extensions). The observed $M_H = 125$ GeV remains consistent with both SM and MSSM but does not decisively confirm either.

# Naturalness and the Hierarchy Problem

- The concept of "naturelessness" (or lack of naturalness) in physics refers to situations where fundamental parameters require extreme fine-tuning to match
- This issue is particularly prominent in the case of the Higgs boson, whose mass appears unnaturally small given the quantum corrections it receives (Hierarchy Problem).
- Hierarchy Problem: Without new physics, the Higgs boson mass is highly sensitive to high-energy scales, leading to severe fine-tuning issues to keep $m_H \sim \Lambda_{EW}$.

- Higgs Mass Sensitivity: In the SM, the Higgs mass receives large radiative corrections:
  - **Fermion Loop (Top Quark):** $\Delta m_H^2 \sim \frac{3|y_t|^2}{8\pi^2}\Lambda^2$
  - **Gauge Boson Loop:** $\Delta m_H^2 \sim \frac{g^2}{16\pi^2}\Lambda^2$
  - **Higgs Self-Interaction:** $\Delta m_H^2 \sim \frac{\lambda}{16\pi^2}\Lambda^2$
- For $\Lambda \sim M_{\text{Planck}}$, corrections are enormous ($\sim 10^{34}$ GeV$^2$), requiring extreme fine-tuning to keep $m_H \sim 125$ GeV.
- Solutions (not exhaustive):
  - **Supersymmetry (SUSY):** Introduces superpartners that cancel quadratic divergences, stabilizing $m_H$.
  - **Composite Higgs Models:** Higgs arises as a bound state from strong interactions.
  - **Extra Dimensions (Randall-Sundrum):** Warped extra dimensions explain the Higgs-Planck hierarchy.

- Supersymmetry and Higgs Mass Stability: SUSY cancels quadratic divergences by introducing superpartners:
  - The stop quark ($\tilde{t}$) cancels top quark loop corrections.
  - The MSSM predicts five Higgs bosons ($h, H, A, H^{\pm}$) instead of one.
  - Radiative corrections raise the lightest (CP- even) Higgs mass, aligning it with the observed 125 GeV.
  - The extended Higgs sector leads to modifications in the couplings between the Higgs bosons and the Standard Model particles. Precision measurements at colliders help constrain these models.
- The unnatural Higgs mass suggests the SM is incomplete. SUSY, extra dimensions, and composite Higgs models provide solutions by reducing fine-tuning. Understanding this remains a central challenge in theoretical physics.

# Feynman Rules

| Interaction | Lagrangian Term | Feynman Rule |
|---|---|---|
| Higgs propagator | $\frac{i}{p^2-m_h^2+i\epsilon}$ | – |
| Higgs-fermion ($hf\bar{f}$) | $-\frac{m_f}{v}h\bar{f}f$ | $-i\frac{m_f}{v}$ |
| Higgs-W boson ($hWW$) | $\frac{m_W^2}{v}hW^{+\mu}W_\mu^-$ | $igm_W g^{\mu\nu}$ |
| Higgs-Z boson ($hZZ$) | $\frac{m_Z^2}{2v}hZ^\mu Z_\mu$ | $i\frac{gm_Z}{\cos\theta_W}g^{\mu\nu}$ |
| Higgs-photon ($h\gamma\gamma$) | Loop-induced | $i\frac{\alpha}{\pi v}F^{\mu\nu}F_{\mu\nu}$ |
| Higgs-gluon ($hgg$) | Loop-induced | $i\frac{\alpha_s}{\pi v}G^{a\mu\nu}G^a_{\mu\nu}$ |
| Higgs trilinear ($hhh$) | $-\frac{3m_h^2}{v}h^3$ | $-i\frac{3m_h^2}{v}$ |
| Higgs quartic ($hhhh$) | $-\frac{3m_h^2}{v^2}h^4$ | $-i\frac{3m_h^2}{v^2}$ |

# Outline

# Higgs Decays

The Higgs Boson is a fundamental particle that interacts more strongly with heavier particles. It's decay patterns help scientists test the Standard Model (SM). If the Higgs decays differently than predicted, it could hint at new physics.

# Decay to Fermions

The decay rate depends on the $m_f$ and includes QCD and electroweak effects. QCD corrections (strong force effects) are calculated using a "running mass" for quarks which changes with energy scale due to the QCD effects. Quark effective masses depend on the energies where they're measured.

The Higgs couples more strongly to heavier particles. The leading order decay width for $h \to f\bar{f}$[4]:

$$\Gamma(h \to f\bar{f}) = \frac{G_F m_f^2 N_c}{4\sqrt{2}\pi} M_h \beta_f^3 \tag{28}$$

Where, $G_F$ is the Fermi constant (strength of weak force), $m_f$ is the mass of the fermion, $N_c$ is the color factor (3 for quarks, 1 for leptons), $M_h$ is the Higgs mass, and $\beta_f$ is the velocity factor, near 1 for light fermions.

[4] arXiv:1808.01324v3

# Including QCD (strong force) effects

Including QCD corrections is important, especially for $h \to b\bar{b}$. A significant portion of the QCD corrections can be accounted for by expressing the decay width in terms of a running mass, $m_f(\mu)$ evaluated at the scale $\mu = M_h$, indicating that the large effects are triggered by large logarithms. The QCD corrected decay width can be approximated as,

$$\Gamma(h \to b\bar{b}) = \frac{3G_F m_b^2 M_h^2}{4\sqrt{2}\pi}\beta_b^3\left(1 + 5.67\frac{\alpha_s(M_h^2)}{\pi} + \cdots\right) \tag{29}$$

Where $\alpha_s(M_h^2)$ is the strong coupling constant defined in the MS-bar scheme with 5 flavors.

# Why mostly $h \to b\bar{b}$ decay?

The Higgs interacts more strongly with heavier particles. The coupling strength is $y_f \sim \frac{m_f}{v}$, where $v$ is the Higgs vacuum expectation value. The bottom quark is the heaviest quark that the Higgs decays into. Higgs doesn't decay into the top quark because $m_t = 173\,\text{GeV}$ which is larger than $M_h/2 = 62.5\,\text{GeV}$, so the Higgs isn't heavy enough to produce two top quarks.

# Higgs decay to weak Bosons (W,Z)

The Higgs is heavy enough to decay to $W^+W^-$ or $ZZ$. However, if $M_h < 2M_W$ or $2M_Z$, one of the bosons is off-shell (i.e., virtual). Over most of the phase space, we can assume that one of the two gauge bosons decays on its mass shell, while the other is pushed into its sizable Breit-Wigner tails. The decay width for such a decay, $h \to ZZ^* \to f_1(p_1)f_2(p_2)Z(p_3)$ is:

$$\Gamma(h \to ZZ^*) = \int_{(M_h-M_Z)^2}^{M_h^2} dm_{12}^2 \int_{m_{23}^2} dm_{23}^2 \frac{|A|^2}{256\pi^3 M_h^3} \tag{30}$$

where $m_{ij} = (p_i + p_j)^2$, and $m_{12}^2 + m_{23}^2 + m_{31}^2 = M_h^2 + M_Z^2$.
The usual Källén function is $\lambda = m_1^4 - 2m_1^2(M_h^2 + M_Z^2) + (M_h^2 - M_Z^2)^2$, and the integration boundaries for $m_{23}^2$ are given by $(M_h^2 + M_Z^2 - m_{12}^2 \pm \sqrt{\lambda})/2$.

The amplitude squared for the decay $h \to Zf\bar{f}$ is given by:

$$|A(h \to Zf\bar{f})|^2 = 32(g_L^2+g_R^2)G_F^2 M_Z^4 \frac{2M_Z^2 m_{12}^2 - m_{13}^2 m_{12}^2 - M_h^2 M_Z^2 + m_{13}^2 M_Z^2 + m_{13}^2 M_h^2 - m_{13}^4}{(m_{12}^2 - M_Z^2)^2 + \Gamma_Z^2 M_Z^2} \tag{31}$$

where $g_L = T_f^3 - Q_f s_W^2$, $g_R = -Q_f s_W^2$, and $T_f^3 = \pm\frac{1}{2}$.
Integrating over $dm_{23}^2$, we find the differential decay rate:

$$\frac{d\Gamma}{dm_{12}^2}(h \to Zf\bar{f}) = \frac{(g_L^2 + g_R^2)G_F^2\sqrt{\lambda}M_Z^4}{48\pi^3 M_h^3} \frac{12M_Z^2 m_{12}^2 + \lambda}{(m_{12}^2 - M_Z^2)^2 + \Gamma_Z^2 M_Z^2} \tag{32}$$

For the decay $h \to Wff'$, the results can be obtained by making the appropriate redefinitions of the fermion-gauge boson couplings. The total decay width for $h \to WW^*$ is:

$$\Gamma(h \to WW^*) = \frac{3g^4 M_h}{512\pi^3} F\left(\frac{M_W}{M_h}\right) \tag{33}$$

For the decay $h \to ZZ^*$, we have:

$$\Gamma(h \to ZZ^*) = \frac{g^4 M_h}{2048 c_W^4 \pi^3} \left(7 - \frac{40}{3} s_W^2 + \frac{160}{9} s_W^4\right) F\left(\frac{M_Z}{M_h}\right) \tag{34}$$

$$\begin{aligned} \text{Here, } F(x) = &- \left|1 - x^2\right| \left[\frac{47}{2} x^2 - \frac{13}{2} + \frac{1}{x^2}\right] \\ &+ 3\left(1 - 6x^2 + 4x^4\right) |\log x| \\ &+ 3\left(1 - 8x^2 + 20x^4\right) \sqrt{4x^2 - 1} \cos^{-1}\left(\frac{3x^2 - 1}{2x^3}\right) \end{aligned}$$

Going beyond the total decay rate and instead studying the $m_{12}$-distribution is a powerful tool in studying the Lorentz structure of the $VVh$ coupling.

# Higgs Decay to Gluons

The decay of the Higgs Boson into two gluons is a loop-induced process in the SM (proceeds through virtual, mainly top, quark loops). This process is closely related to Higgs production via gluon fusion ($gg \to h$), since same effective Higgs-gluon coupling involved. The decay width for $h \to gg$ is:

$$\Gamma(h \to gg) = \frac{G_F \alpha_s^2 M_h^3}{64\sqrt{2}\pi^3} \sum_q F_{1/2}(\tau_q)^2 \tag{35}$$

where $G_F$ is the Fermi constant, $\alpha_s$ is the strong coupling constant, $\tau_q = \frac{4m_q^2}{M_h^2}$, and $F_{1/2}(\tau_q)$ is the loop function for spin $\frac{1}{2}$.

The loop function encodes the quantum corrections from virtual quarks and is defined as:

$$F_{1/2}(\tau_q) \equiv -2\tau_q \left[1 + (1-\tau_q) f(\tau_q)\right] \tag{36}$$

It includes one power of the Yukawa coupling, expressed in terms of the mass, and the rescaled scalar one-loop three-point function:

$$f(\tau_q) = \begin{cases} \sin^{-1}\left(\sqrt{\frac{1}{\tau_q}}\right)^2 & \text{for } \tau_q \geq 1 \\ -\frac{1}{4}\left[\log\left(\frac{1+\sqrt{1-\tau_q}}{1-\sqrt{1-\tau_q}}\right) - i\pi\right]^2 & \text{for } \tau_q < 1 \end{cases} \tag{37}$$

# Dominant Contribution

Top quark ($t$): Since $m_t \gg M_h/2$, the top quark dominates the loop contribution. In the limit $\tau_t \to \infty$ (very heavy top), the loop function approaches $F_{1/2}(\tau_t) \to -4/3$. This shows non-decoupling behavior even if the top quark still contributes significantly because its Yukawa coupling compensates for its large mass.
For the light quarks such as bottom ($b$), $M_q \ll M_h$. The loop function is:

$$F_{1/2}(\tau_b) \to \frac{2m_b^2}{M_h^2} \log^2\left(\frac{4m_b^2}{M_h^2}\right) \tag{38}$$

This contribution is suppressed due to the small mass.

# Higgs decay to Photons

The decay $h \to \gamma\gamma$ is a loop-induced process since the Higgs Boson doesn't couple directly to photons at tree level. The dominant contribution comes from:

1. Fermion loops (especially the top quark due to its large Yukawa coupling)
2. $W$-Boson loops (electroweak gauge bosons)
3. Possible Beyond Standard Model (BSM) scalar contribution

The decay width is:

$$\Gamma(h \to \gamma\gamma) = \frac{\alpha^2 G_F}{128\pi^3} M_H^3 \left| \sum_f N_{c,f} Q_f^2 F_{1/2}^{(f)} + F_1(\tau(W)) + \sum_S N_{c,S} \frac{g_{hSS}}{m_S^2} F_0(\tau(S)) \right|^2 \tag{39}$$

Where $\alpha$ is the fine structure constant, $Q_f$ is the electric charge of fermions, $\tau_i = \frac{4m_i^2}{M_h^2}$ (for $i = f, W, S$), and $F_{1/2}, F_1, F_0$ are the loop functions for fermions, $W$-bosons, and scalars respectively.
The scalar loop function $F_{1/2}(\tau_q)$ is given in Eq. (9), and

$$F_1(\tau_W) = 2 + 3\tau_W \left[1 + (2 - \tau_W) f(\tau_W)\right],$$

$$F_0(\tau_S) = \tau_S \left[1 - \tau_S f(\tau_S)\right].$$

# Loop Functions

- Fermion loop function $F_{1/2}$: It is given by the same expression as in the gluon fusion case (Eqn 9). In the heavy mass limit ($\tau_f \to \infty$), $F_{1/2} = 4/3$.
- $W$-Boson loop function $F_1$: First equation of the above. In the heavy mass limit ($\tau_W \to \infty$), $F_1 = 7$.
- Scalar loop function $F_0$ (for BSM scalars): Second equation of the above. In the heavy mass limit ($\tau_s \to \infty$), $F_0 = -1/3$.

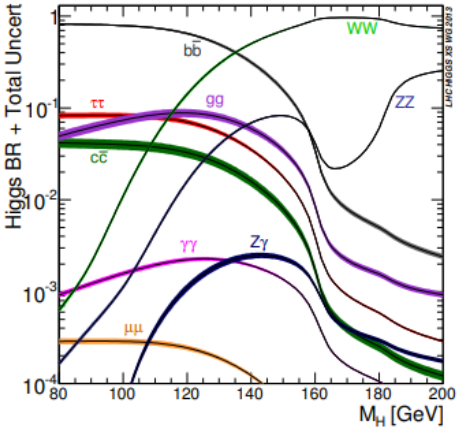


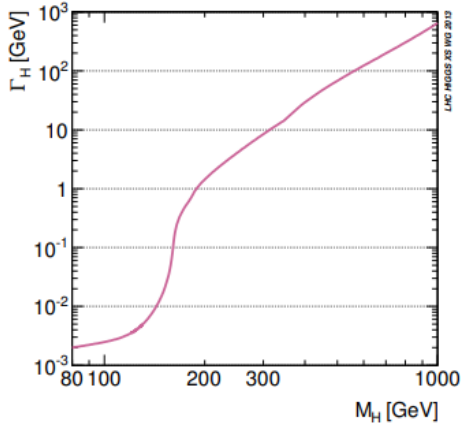


Figure: Left: SM Higgs branching ratios. The widths of the curves are estimates of the theoretical uncertainty. Right: Total width for a SM-like Higgs boson of arbitrary mass.[5]

[5] arXiv:107.5909

# Outline

# Where do we look?

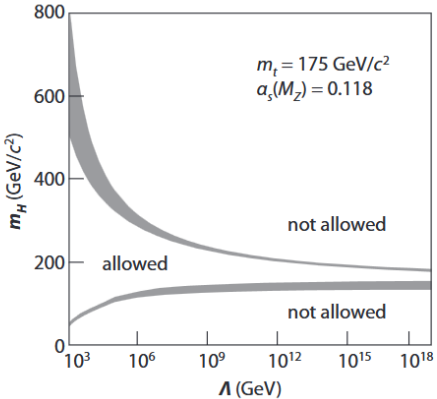


Figure: Lower and upper limits on the Higgs boson mass as a function of the cut-off energy scale $\Lambda$, relying on the vacuum stability (lower band) and triviality (upper band) arguments

# Pre-LEP Era (before 1989)

Masses $< 5$ GeV$/c^2$ were unlikely. Experiments active were:

1. SINDRUM Spectrometer at the PSI 590 MeV proton cyclotron.[6]
2. CERN-Edinburgh-Mainz-Orsay-Pisa-Siegen collaboration at CERN SPS[7]
3. CLEO[8]
4. CUSB Collaboration[9]

[6] SciPost Phys. Proc. 5, 007 (2021)
[7] Physics Letters B, Volume 235, Issues 3–4, 1990, 356-362
[8] Physical Review D. 40 (3): 712–720.
[9] Physical Review D. 33 (1): 300–302

# Need for better searches

The searches described so far were sensitive to potentially large QCD corrections. We required unabiguous searches in the low mass region.

# LEP1 Era

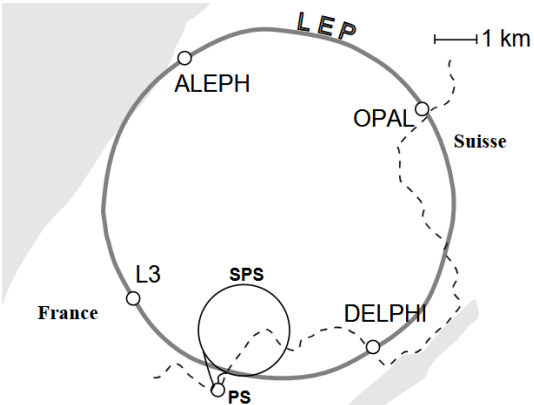


Figure: Overview of the LEP collider [10]

[10] Muijs, Sandra & Duinker, Pieter. Tau pair production above the Z resonance.

# Accelerators at CERN

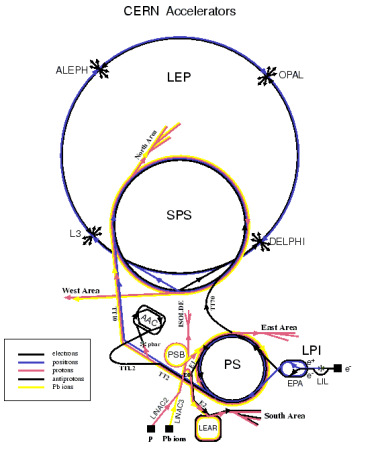

# Production Mechanisms (at the Z resonance)

The expected mechanisms were the Bjorken and Wilczek processes. However the production rate in the Wilczek process is lower and heavy backgrounds make it unfeasible.

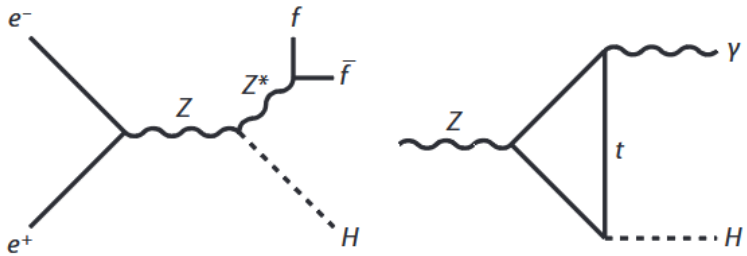


Figure: (left) Bjorken process, (right) Wilczek process

# Low mass searches

| Higgs boson mass range[11] | Primary decay products |
|---|---|
| $m_H < 2m_e$ | $\gamma\gamma$ |
| $2m_e < m_H < 2m_\mu$ | $e^+e^-$ |
| $2m_\mu < m_H < 2m_\pi$ | $\mu^+\mu^-$ |
| $2m_\pi < m_H < (2 - 3\text{GeV}/c^2)$ | hadron pair |
| PQCD domain $< b\bar{b}$ threshold | heaviest available fermion pair ($c\bar{c}$ or $\tau^+\tau^-$) |
| Above $b\bar{b}$ threshold | $b\bar{b}$ |

[11] Decamp D, et al. (ALEPH Collab.). Phys. Lett. B 236:233 (1990)

# The Higgs boson mass and QCD

Non-perturbative $\rightarrow$ perturbative QCD at $m_H \approx 2\text{GeV}/c^2$, indicated by smooth variation of BR above this mass.[12]

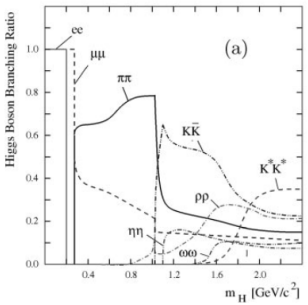


Figure: Branching ratios of Higgs boson for low mass Higgs[13]

[12] Janot P. LAL 89–45 (1989), Decamp D, et al. (ALEPH Collab.). Phys. Lett. B 236:233 (1990)

[13] Annu. Rev. Nucl. Part. Sci. 2002.52:65-113

# Searches

For $m_H < 20\text{GeV}/c^2$, over 10,000 events expected at LEP1 from Higgstrahlung ($e^+e^- \to Z^* \to ZH$). Number of observed events agreed with SM and $m_H < 20\text{GeV}/c^2$ excluded at 95% CL.
Decays of $Z^*$ were studied, but excessive hadronic backgrounds present. Low production rate ($< 40$ events) prohibits study of decays into hadrons and taus. So only the $Z^* \to \nu\nu, \mu\mu, ee$ were studied. These make up 25% of decays (10 events in 13 million hadronic decays collected at LEP by all 4 experiments).

$m_H$ constraint:

Combined results gave lower limit 65.6 $\text{GeV}/c^2 < m_H$[14].

[14] LEP Higgs Working Group, http://lephiggs.web.cern.ch/LEPHIGGS

# LEP2 runs

In 1996, direct searches for on-shell diboson production ($ZH$) began, as LEP increased $\sqrt{s} \to 160$ GeV
By 2000, $\sqrt{s} = 209$ GeV attained.

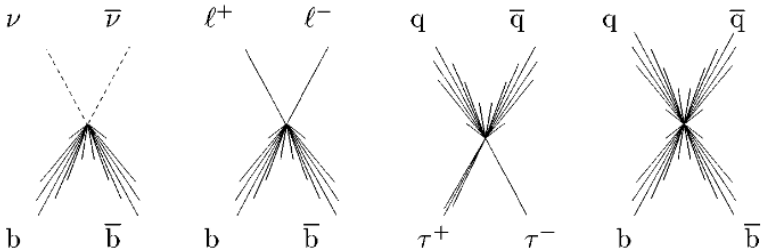


Figure: Topologies involved in the search for the standard-model Higgs boson at LEP2, missing energy, lepton pairs, $\tau^+\tau^-$, four-jets.[15]

[15] Annu. Rev. Nucl. Part. Sci. 2002.52:65-113

# Why didn't we find the Higgs at LEP?

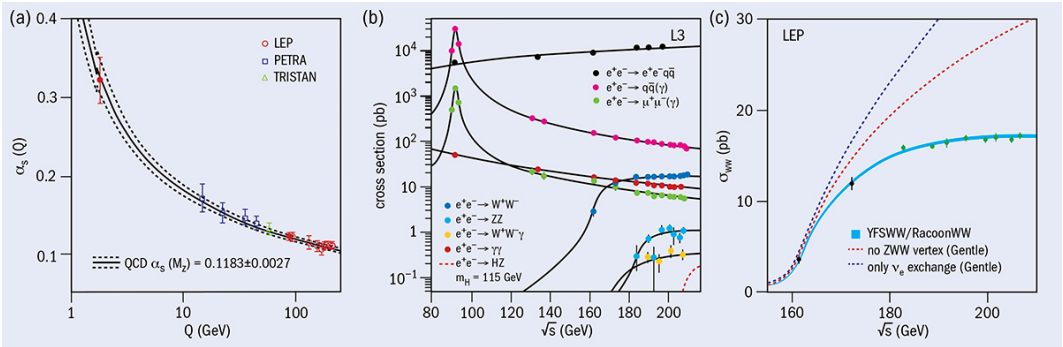


Figure: Measurements of various $ee \to X$ cross section by L3 at LEP. Note the low $\sigma(ee \to HZ)$ values.

# Why didn't we find the Higgs at LEP?

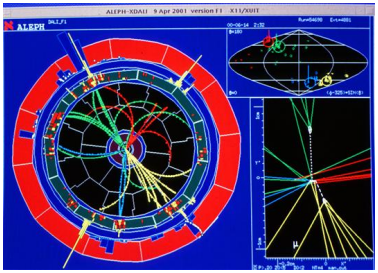


Figure: (CERN-EX-0106015, 14/06/2000) "This track is an example of real data collected from the ALEPH detector on the Large Electron-Positron (LEP) collider at CERN, which ran between 1989 and 2000. Four jets of hadrons can be seen in the detector that could have resulted from the associated production and decay of a Z0 and a Higgs boson into quark-antiquark pairs, which appear in the detector as jets of hadrons. However, other processes can produce similiar tracks so this is not conclusive evidence for the Higgs."

# ALEPH's tracks

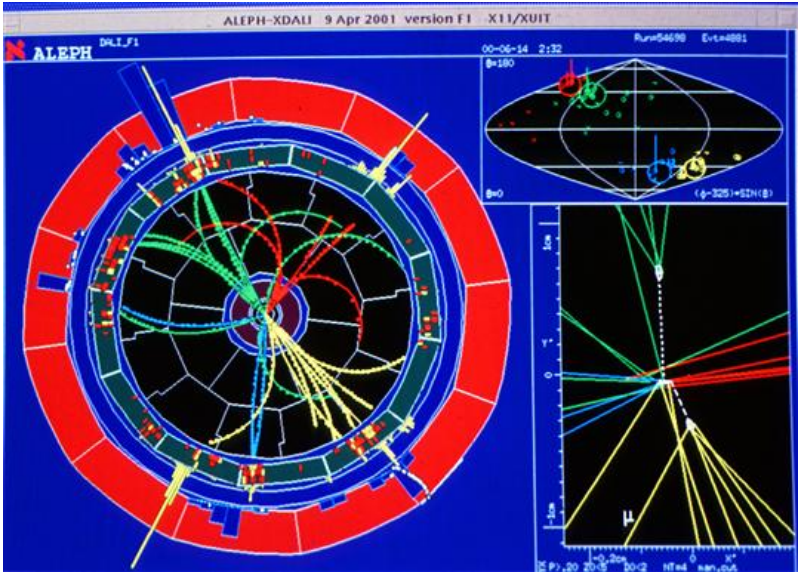

# Why didn't the TeVatron find the Higgs?

While they didn't conclusively find it, they did see the Higgs boson.[16]

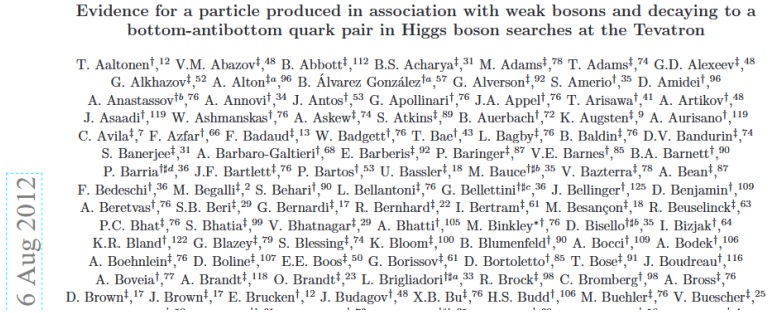

**Evidence for a particle produced in association with weak bosons and decaying to a bottom-antibottom quark pair in Higgs boson searches at the Tevatron**


T. Aaltonen[†,12] V.M. Abazov[‡,48] B. Abbott[‡,112] B.S. Acharya[‡,31] M. Adams[‡,78] T. Adams[‡,74] G.D. Alexeev[‡,48] G. Alkhazov[‡,52] A. Alton[‡a,96] B. Álvarez González[‡a,57] G. Alverson[‡,92] S. Amerio[†,35] D. Amidei[†,96] A. Anastassov[‡b,76] A. Annovi[†,34] J. Antos[†,53] G. Apollinari[‡,76] J.A. Appel[‡,76] T. Arisawa[‡,41] A. Artikov[‡,48] J. Asaadi[†,119] W. Ashmanskas[‡,76] A. Askew[‡,74] S. Atkins[‡,89] B. Auerbach[†,72] K. Augsten[‡,9] A. Aurisano[†,119] C. Avila[‡,7] F. Azfar[†,66] F. Badaud[‡,13] W. Badgett[†,76] T. Bae[†,43] L. Bagby[‡,76] B. Baldin[‡,76] D.V. Bandurin[‡,74] S. Banerjee[‡,31] A. Barbaro-Galtieri[†,68] E. Barberis[‡,92] P. Baringer[‡,87] V.E. Barnes[‡,85] B.A. Barnett[†,90] P. Barria[‡‡d,36] J.F. Bartlett[‡,76] P. Bartos[†,53] U. Bassler[‡,18] M. Bauce[‡‡b,35] V. Bazterra[‡,78] A. Bean[‡,87] F. Bedeschi[†,36] M. Begalli[‡,2] S. Behari[†,90] L. Bellantoni[‡,76] G. Bellettini[‡‡c,36] J. Bellinger[†,125] D. Benjamin[†,109] A. Beretvas[†,76] S.B. Beri[‡,29] G. Bernardi[‡,17] R. Bernhard[‡,22] I. Bertram[‡,61] M. Besançon[‡,18] R. Beuselinck[‡,63] P.C. Bhat[‡,76] S. Bhatia[‡,99] V. Bhatnagar[‡,29] A. Bhatti[†,105] M. Binkley*[†,76] D. Bisello[‡‡b,35] I. Bizjak[†,64] K.R. Bland[†,122] G. Blazey[‡,79] S. Blessing[‡,74] K. Bloom[‡,100] B. Blumenfeld[†,90] A. Bocci[†,109] A. Bodek[†,106] A. Boehnlein[‡,76] D. Boline[‡,107] E.E. Boos[‡,50] G. Borissov[‡,61] D. Bortoletto[†,85] T. Bose[‡,91] J. Boudreau[†,116] A. Boveia[†,77] A. Brandt[†,118] O. Brandt[‡,23] L. Brigliadori[‡‡a,33] R. Brock[‡,98] C. Bromberg[†,98] A. Bross[‡,76] D. Brown[‡,17] J. Brown[‡,17] E. Brucken[†,12] J. Budagov[†,48] X.B. Bu[‡,76] H.S. Budd[†,106] M. Buehler[‡,76] V. Buescher[‡,25]



6 Aug 2012


[16] Aaltonen et al., 1207.6436, 2012

# The *CDF* and $D^0$'s findings

- Data obtained from Fermilab's Tevatron $p\bar{p}$ collisions at $\sqrt{s} = 1.96$ TeV. integrated luminosities upto 9.7 $\text{fb}^{-1}$
- Searches conducted in $100 - 150$ $\text{GeV}/c^2$ range.
- Excess observed between $120 - 135$ $\text{GeV}/c^2$ with global significance of $3.1\sigma$.

# The Tevatron data

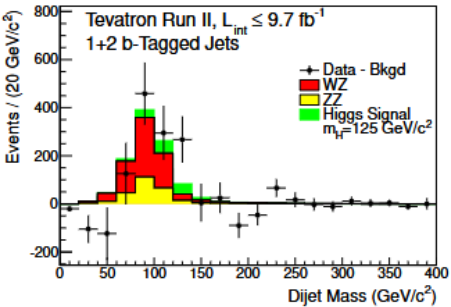


Figure: Background-subtracted distribution of the reconstructed dijet mass $m_{jj}$ , summed over all input channels[17]

[17] Aaltonen et al, 2012

# Branching ratios

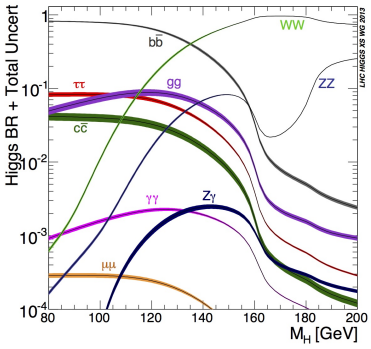


Figure: Branching ratios of Higgs v/s $m_H$[18]

[18]P.A. Zyla et al. (Particle Data Group), Prog. Theor. Exp. Phys. 2020, 083C01 (2020)

# $H \to b\bar{b}$ is difficult to distinguish

| Experiment | $\mu = \sigma/\sigma_{SM}$ | Expected significance |
|---|---|---|
| CDF | $2.5 \pm 1.0$ | $1.3\,\sigma$ [17] |
| D0 | $1.2 \pm 1.1$ | $1.5\,\sigma$ [18] |
| D0+CDF | $1.95 \pm 0.75$ | $1.9\,\sigma$ [16] |
| ATLAS | $0.2 \pm 0.9$ | $1.6\,\sigma$ [19] |
| CMS | $1.0 \pm 0.5$ | $2.1\,\sigma$ [8] |

Figure: Signal strength and expected significance for the VH searches at Tevatron and LHC colliders.[19]

[19] Search for the Higgs boson in the $\bar{b}b$ decay channel using the CMS detector, 2014

# Jets and backgrounds

At $m_H = 125\ \text{GeV}/c^2, H \to b\bar{b}$ is the primary decay. b-quarks hadronize and we see 'jets', which are not clean signatures. In a hardon collider, backgrounds are immense!

So how do you resolve this?

Look for 'cleaner' signatures: $H \to ZZ, \gamma\gamma$, with BRs $2.67\%, 0.228\%$. Tevatron couldn't provide enough data for this. On to the LHC.

# The Large Hadron Collider

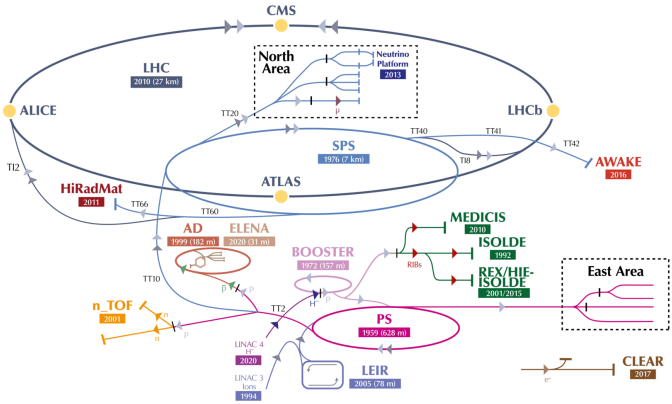


Figure: The CERN accelerator complex layout in 2022[20]

[20] Landua, Fabienne, The CERN accelerator complex layout in 2022, 2022

# The ATLAS Detector

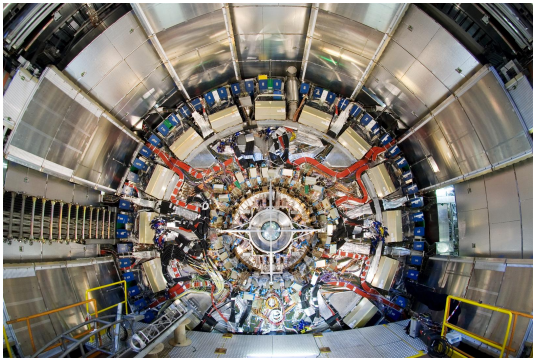

Figure: "ATLAS has the dimensions of a cylinder, 46m long, 25m in diameter, and sits in a cavern 100m below ground. The ATLAS detector weighs 7,000 tonnes, similar to the weight of the Eiffel Tower."

# Preliminaries I: Bunch-crossing

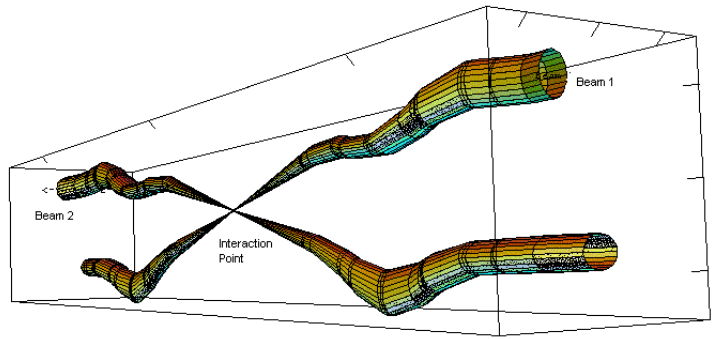


Figure: Bunch crossing/ pileup: 100,000 million protons per bunch squeezed down to 64 microns in ATLAS. Bunches cross every $\approx 25$ ns.[21]

[21] Collisions, https://lhc-machine-outreach.web.cern.ch/collisions.htm

# Preliminaries II: Pseudorapidity

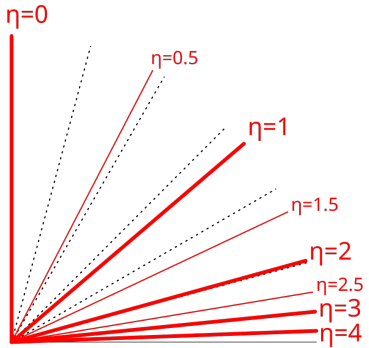


Pseudorapidity $\eta = -\ln\left[\tan\left(\frac{\theta}{2}\right)\right]$

# ATLAS component coverages

1. Electromagnetic calorimeter
   - Central barrel $|\eta| < 1.475$
   - Outer wheel $1.375 < |\eta| < 2.5$
   - Inner wheel $2.5 < |\eta| < 3.2$
2. Inner detector $|\eta| < 2.5$
3. Forward region (LAr calorimeters) $3.2 < |\eta| < 4.9$

$l, \gamma$ measurements precisely done in $|\eta| < 2.5$. Jets and $E_T^{miss}$ reconstructed through full coverage $|\eta| < 4.9$

# First glimpses, December 12, 2011

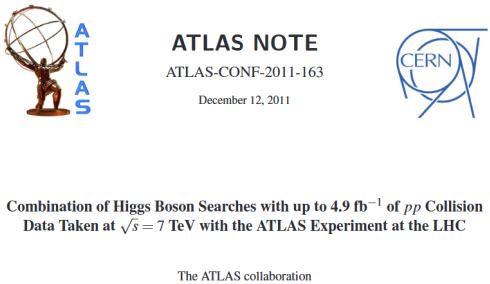


Figure: An initial look by ATLAS on what might be the Higgs boson

# First glimpses, February 7, 2012

- The first conference article was followed up immediately by another.[22]
- Gluon-gluon fusion was considered to be the primary production mechanism.
- Processes considered: $H \to \gamma\gamma, H \to ZZ^* \to l^+l^-l'^+l'^-, H \to ZZ \to l^+l^-q\bar{q}, H \to ZZ \to l^+l^-\nu\bar{\nu}, H \to WW^* \to l^+\nu l'^-\bar{\nu}, H \to WW \to l\nu q\bar{q}'$
- Quantified an excess of events around $m_H = 126$ GeV

[22] Combined search for the Standard Model Higgs boson using up to $4.9 fb^{-1}$ of pp collision data at $\sqrt{s} = 7$ TeV with the ATLAS detector at the LHC, 2012

# Initial data

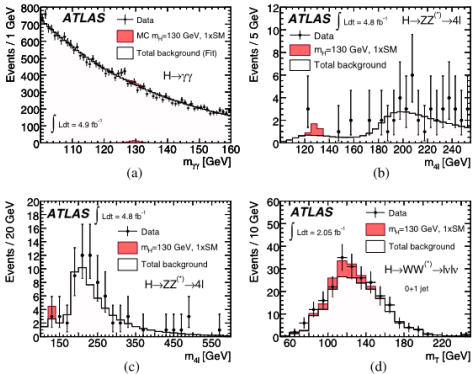


Figure: Distributions of the reconstructed invariant or transverse mass for the selected candidate events and for the total background and signal ($m_H = 130$ GeV) expected in $H \to \gamma\gamma$(a), the $H \to ZZ^* \to l^+l^-l'^+l'^-$ in the low mass region (b) and the entire mass range (c), and the $H \to WW^* \to l^+\nu l'^-\bar{\nu}$ (d) channels.

# We find the Higgs, July 4, 2012

## Observation of a new particle in the search for the Standard Model Higgs boson with the ATLAS detector at the LHC ☆

ATLAS Collaboration *

This paper is dedicated to the memory of our ATLAS colleagues who did not live to see the full impact and significance of their contributions to the experiment.

ARTICLE INFO

*Article history:*
Received 31 July 2012
Received in revised form 8 August 2012
Accepted 11 August 2012
Available online 14 August 2012
Editor: W.-D. Schlatter

ABSTRACT

A search for the Standard Model Higgs boson in proton–proton collisions with the ATLAS detector at the LHC is presented. The datasets used correspond to integrated luminosities of approximately 4.8 fb$^{-1}$ collected at $\sqrt{s} = 7$ TeV in 2011 and 5.8 fb$^{-1}$ at $\sqrt{s} = 8$ TeV in 2012. Individual searches in the channels $H \to ZZ^{(*)} \to 4\ell$, $H \to \gamma\gamma$ and $H \to WW^{(*)} \to e\nu\mu\nu$ in the 8 TeV data are combined with previously published results of searches for $H \to ZZ^{(*)}$, $WW^{(*)}$, $b\bar{b}$ and $\tau^+\tau^-$ in the 7 TeV data and results from improved analyses of the $H \to ZZ^{(*)} \to 4\ell$ and $H \to \gamma\gamma$ channels in the 7 TeV data. Clear evidence for the production of a neutral boson with a measured mass of $126.0 \pm 0.4$ (stat) $\pm 0.4$ (sys) GeV is presented. This observation, which has a significance of 5.9 standard deviations, corresponding to a background fluctuation probability of $1.7 \times 10^{-9}$, is compatible with the production and decay of the Standard Model Higgs boson.

# Details of the search

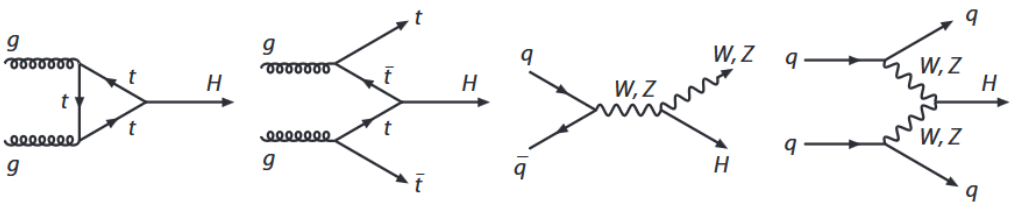


Figure: SM Higgs boson production processes considered in the analysis.

# Details of the search[23]

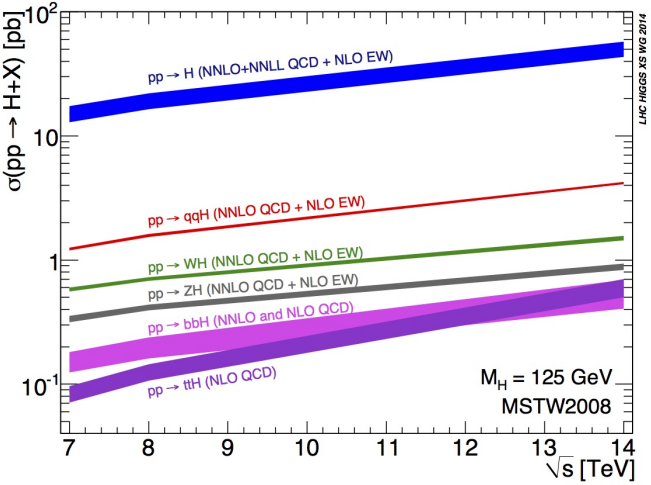


[23]P.A. Zyla et al. (Particle Data Group), Prog. Theor. Exp. Phys. 2020, 083C01 (2020)

# Simulators utilised

**Table 1**
Event generators used to model the signal and background processes. "PYTHIA" indicates that PYTHIA6 and PYTHIA8 are used for simulations of $\sqrt{s} = 7$ TeV and $\sqrt{s} = 8$ TeV data, respectively.

| Process | Generator |
|---|---|
| ggF, VBF | POWHEG [57,58] + PYTHIA |
| $WH$, $ZH$, $t\bar{t}H$ | PYTHIA |
| $W$ + jets, $Z/\gamma^*$ + jets | ALPGEN [59] + HERWIG |
| $t\bar{t}$, $tW$, $tb$ | MC@NLO [60] + HERWIG |
| $tqb$ | AcerMC [61] + PYTHIA |
| $q\bar{q} \to WW$ | MC@NLO + HERWIG |
| $gg \to WW$ | gg2WW [62] + HERWIG |
| $q\bar{q} \to ZZ$ | POWHEG [63] + PYTHIA |
| $gg \to ZZ$ | gg2ZZ [64] + HERWIG |
| $WZ$ | MadGraph + PYTHIA, HERWIG |
| $W\gamma$ + jets | ALPGEN + HERWIG |
| $W\gamma^*$ [65] | MadGraph + PYTHIA |
| $q\bar{q}/gg \to \gamma\gamma$ | SHERPA |

# Decay channel details, I

| Channel | Event selection |
|---|---|
| $H \to ZZ^{(*)} \to 4l$ | single and dilepton triggers, $\Delta R$ constraints, transverse impact parameter, isolation requirements |
| $H \to \gamma\gamma$ | diphoton trigger, track requirements, shower shapes |
| $H \to WW^{(*)} \to e\nu\mu\nu$ | large $E_T^{miss}$, opposite charge leptons, single lepton triggers, stringent isolation requirements, jet multiplicities |

# Decay channel details, II

| Channel | Background estimation |
|---|---|
| $H \to ZZ^{(*)} \to 4l$ | MC simulation, normalized to $\sigma(ZZ^{(*)})$;<br>Z+jets, $t\bar{t}$ (for $ll + \mu\mu$);<br>selection criteria, etc. |
| $H \to \gamma\gamma$ | Drell-Yan processes, $\gamma j, jj$, etc. divided into 10 mutually exclusive categories |
| $H \to WW^{(*)} \to e\nu\mu\nu$ | W+jets, $W\gamma^{(*)}$, $t \to Wb$, WW |

# Final data

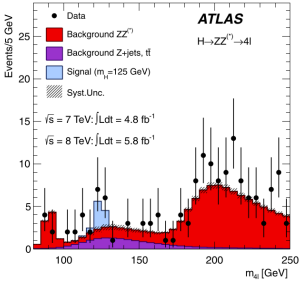


(a) 4$l$ invariant mass distributions

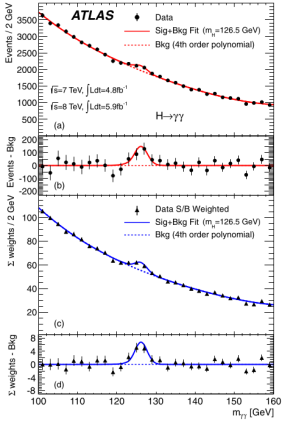


(b) 4$l$ invariant mass distributions

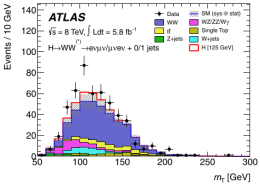


(c) 4$l$ invariant mass distributions

# Combined data

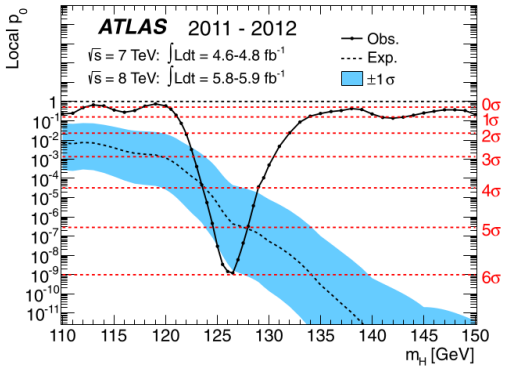


Figure: Observed local $p_0$ as a function of $m_H$

# Conclusive results of the Higgs boson

The ATLAS collaboration hence gave conclusive evidence for the discovery of a new particle with mass $126.0 \pm 0.4(\text{stat}) \pm 0.4(\text{sys})$ GeV. Decay to pairs of vector boson indicated the charge neutrality of the particle. Diphoton channel disfavored the spin-1 hypothesis.

### CMS Collaboration

Simultaneously found the Higgs, with a mass $m_H = 125.3 \pm 0.4(\text{stat}) \pm 0.5(\text{sys})$ GeV.

### Joint measurements by CMS and ATLAS (2015)

$m_H = 125.09 \pm 0.21(\text{stat}) \pm 0.11(\text{sys})$ GeV.

This value is consistent with SM predictions and ensures the stability of electroweak theory.

# A map of Higgs boson interactions[24]

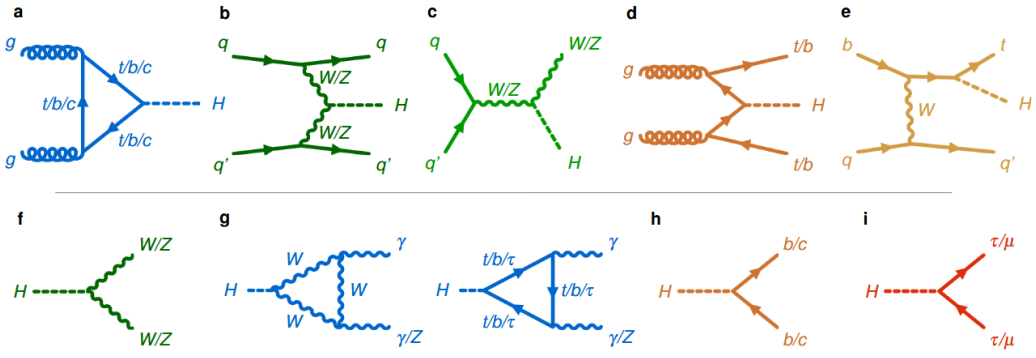


[24] The ATLAS Collaboration. A detailed map of Higgs boson interactions by the ATLAS experiment ten years after the discovery. Nature 607, 52–59 (2022). https://doi.org/10.1038/s41586-022-04893-w

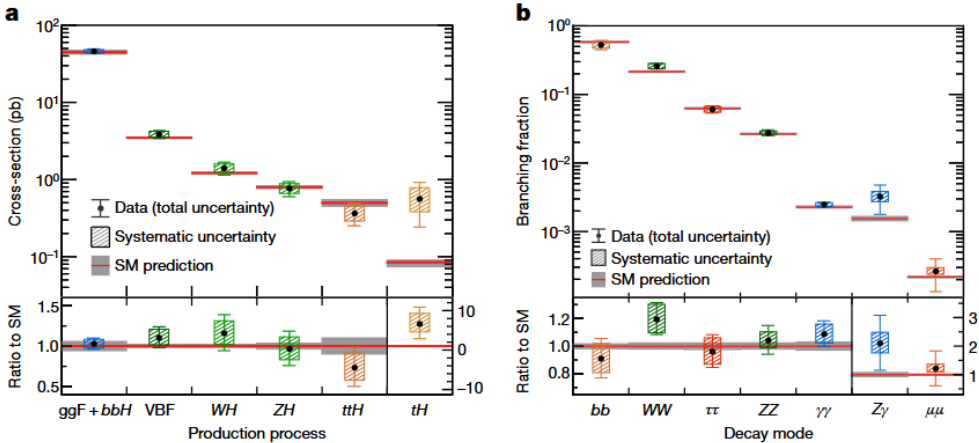


Figure: Production rates and decay BRs and ratios to SM expectations, p-values for SM compatibility are $a$ : 65%, $b$ : 56%

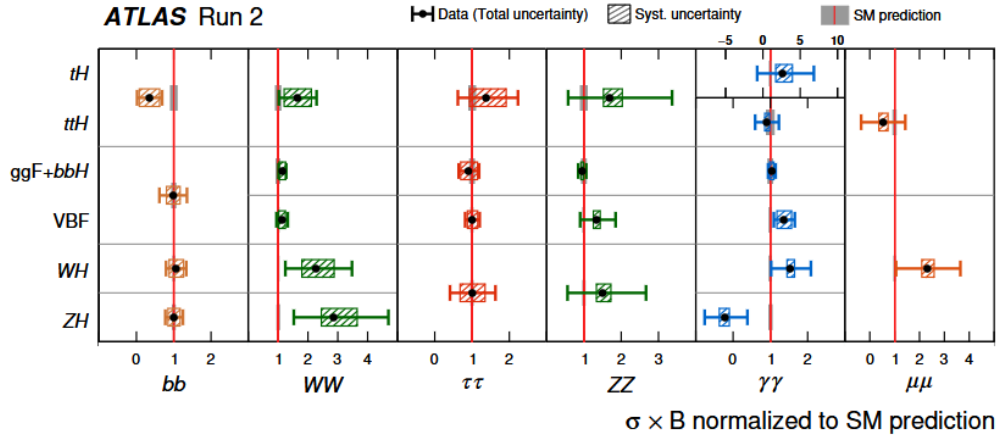


Figure: Ratio of observed rate to predicted SM event rate for different combinations of Higgs boson production and decay processes

# Signal strength measures

Using $\sigma_i$ as cross-section and $B_f$ as branching fraction for a production process $i$ and decay channel $f$ respectively, ATLAS defines the signal strength modifier:

$$\mu_{if} = \frac{\sigma_i}{\sigma_i^{SM}} \times \frac{B_f}{B_f^{SM}} \tag{40}$$

Assuming that all processes have a global signal strength $\mu = \mu_{if}$, ATLAS determined:

$$\mu = 1.05 \pm 0.06 = 1.05 \pm 0.03\ (\text{stat.}) \pm 0.03\ (\text{exp.}) \pm 0.04\ (\text{sig. th.}) \pm 0.02(\text{bkg. th.})$$

# $\kappa$-definitions

Utilising the structure of Yukawa coupling to Higgs, we define reduced coupling strength modifiers:

$$\sqrt{\frac{\kappa_V g_V}{2\text{vev}}} = \sqrt{\kappa_V}\frac{m_V}{\text{vev}}; \quad \kappa_F g_F = \frac{\kappa_F m_F}{\text{vev}}$$

# $\kappa$-measurements

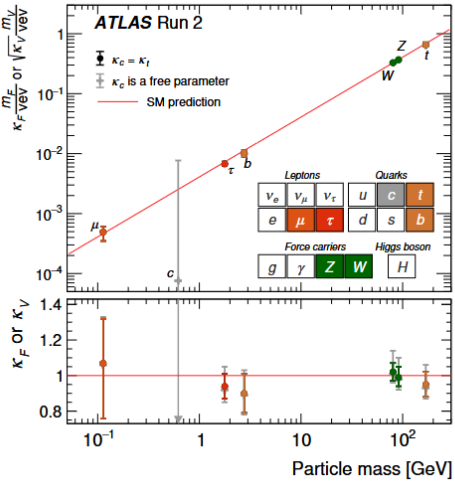


Figure: Reduced Higgs boson coupling strength modifiers and their uncertainties

# $\kappa$ per particle type

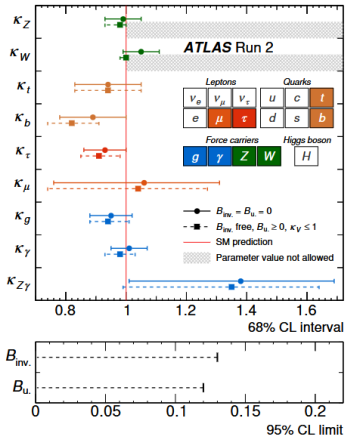


Figure: Reduced coupling strength modifiers and their uncertainties per particle type with effective photon, $Z\gamma$ and gluon couplings

# Outline

# Higgs Decay Width and Lifetime

If the width is larger than predicted, it could imply:

- New decay channels (e.g., Higgs decaying to invisible dark matter).
- Exotic interactions beyond SM.

If the width is smaller, it would imply suppressed couplings or new physics effects. The width $\Gamma_h$ measures how quickly Higgs decays. In the SM, for $M_h \sim 125$ GeV, the predicted width is:

$$\Gamma_h \sim 4 \text{ MeV} \tag{41}$$

This is extremely narrow compared to the detector resolution ($\sim$1 GeV), making direct measurement difficult.

# Challenges in Measuring the Width

LHC cannot directly measure $\Gamma_h$ due to limited detector resolution. Instead, indirect methods are used, such as:

- Interference effects (e.g., $gg \to H \to ZZ$ vs $gg \to ZZ$ background).
- Off-shell vs on-shell Higgs production.

Future colliders like FCC, ILC may achieve better precision.

# Challenges and Assumptions

The Higgs coupling to gluons is loop-induced and can have a non-trivial dependence on all masses involved. Thus, extracting the Higgs width requires assuming that:

- All interactions are those of the SM.
- No exotic decays or new physics contributions exist.

# Future Improvements

- High Luminosity LHC (HL-LHC): more data will reduce uncertainties.
- Future lepton colliders (FCC-ee, ILC) could measure the width directly via Higgsstrahlung with better precision.

# Spin

Since no visible renormalizable theories predict alternative Higgs spin, physicists used an effective Lagrangian to test different spin/CP hypotheses. The effective interactions that were used to constrain such couplings or to contrast with the SM Higgs in simple hypothesis tests need to be understood as straw-man proposals. They are not motivated by the actual models and they typically cannot be understood in terms of renormalizable theories.

# Possible Spin Hypotheses

Spin-0 (scalar/pseudoscalar): CP-even (scalar, like SM Higgs)

$$L^{j=0} = g_1^{(0)} h V^{\mu} V_{\mu} - \frac{g_2^{(0)}}{4} h V^{\mu\nu} V_{\mu\nu} - \frac{g_3^{(0)}}{4} A V^{\mu\nu} \widetilde{V_{\mu\nu}} - \frac{g_4^{(0)}}{4} h G^{\mu\nu} G_{\mu\nu} - \frac{g_5^{(0)}}{4} A G^{\mu\nu} \widetilde{G_{\mu\nu}} \tag{42}$$

Spin-1 (Vector boson): Ruled out early because spin-1 predicts different angular correlations $H \to \gamma\gamma$ and $H \to ZZ$.

$$
\begin{aligned}
L^{j=1} = & ig_1^{(1)} \left( W^+_{\mu\nu} W^{-\mu} - W^-_{\mu\nu} W^{+\mu} \right) Y^{(e)\nu} + ig_2^{(1)} W^+_\mu W^-_\nu Y^{(e)\mu\nu} + g_3^{(1)} \epsilon^{\mu\nu\rho\sigma} \\
& \left( W^+_\mu \overleftrightarrow{\partial}_\rho W^-_\nu \right) Y^{(e)}_\sigma + ig_4^{(1)} \tilde{W}^+_{\sigma\mu} W^{-\mu\nu} Y^{(e)\sigma}_\nu - g_5^{(1)} W^+_\mu W^-_\nu \\
& \left( \partial^\mu Y^{(o)\nu} + \partial^\nu Y^{(o)\mu} \right) + ig_6^{(1)} W^+_\mu W^-_\nu \tilde{Y}^{(o)\mu\nu} + ig_7^{(1)} \tilde{W}^+_{\sigma\mu} W^{-\mu\nu} \tilde{Y}^{(o)\sigma}_\nu \\
& + g_8^{(1)} \epsilon^{\mu\nu\rho\sigma} Y^{(e)}_\mu Z_\nu (\partial_\rho Z_\sigma) + g_9^{(1)} Y^{(o)}_\mu (\partial_\nu Z^\mu) Z^\nu
\end{aligned}
\tag{43}
$$

Spin-2 (Tensor particle): Couples via the energy-momentum tensor.

$$
L^{j=2} = -g_1^{(2)} G^{\mu\nu} T_{\mu\nu V} - g_2^{(2)} G^{\mu\nu} T_{\mu\nu G} - g_3^{(2)} G^{\mu\nu} T_{\mu\nu f} \tag{44}
$$

### Spin-0 v/s Spin-2 Discrimination

ATLAS and CMS compared $h \to ZZ^* \to 4l$ angular distributions, where spin-2 predicts a different $\cos\theta^*$ dependence than spin-0. Data strongly favors spin-0 (Figure below, right).

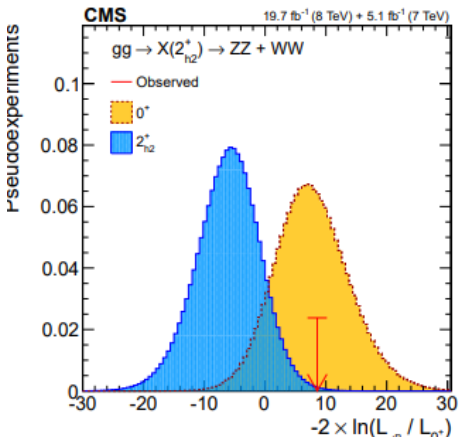


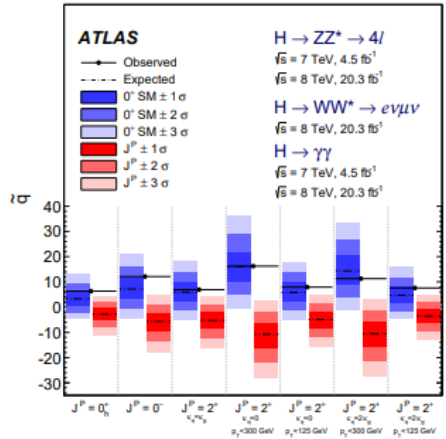


Figure: Left: comparison of CP-even vs. CP-odd scalar hypotheses, right: comparisons of various alternate hypothesis against the SM Higgs boson[25]

[25] arXiv:1506.05669

# CP Even vs CP Odd Tests

A pseudoscalar Higgs, which is CP-odd, would have different $h \to \tau\tau$ decay distributions. Moreover, opposite $h \to \gamma\gamma$ polarization effects could arise. However, experimental findings indicate that the Higgs is mostly CP-even, but small CP-odd admixtures are still allowed ( 10-20%).

# Spin-1 Exclusion

Spin-1 predicts forbidden decay modes, for example, $H \to \gamma Z$, which can vanish in spin-0 but not in spin-1. LHC data excludes pure spin-1 at greater than 99.9% confidence level.

# Constraining Higgs Spin and CP Properties

Higgs boson's spin and CP properties by studying its decay angular distributions. This is done by analyzing the kinematics of decays like $X \to WW, ZZ$ where $X$ is the Higgs or an imposter.
To distinguish between different spin/CP hypotheses, we define reference frames and angles in a following figure. Now, let us define the kinematic variables:

$$\vec{p}_{Zh} = \vec{p}_{\alpha} + \vec{p}_{\beta} \quad \text{(Z from h decay)}$$
$$\vec{p}_{Zl} = \vec{p}_{+} + \vec{p}_{-} \quad \text{(Z leptonic decay)}$$
$$\vec{p}_{X} = \vec{p}_{Zh} + \vec{p}_{Zl} \quad \text{(Total Higgs Momentum)}$$

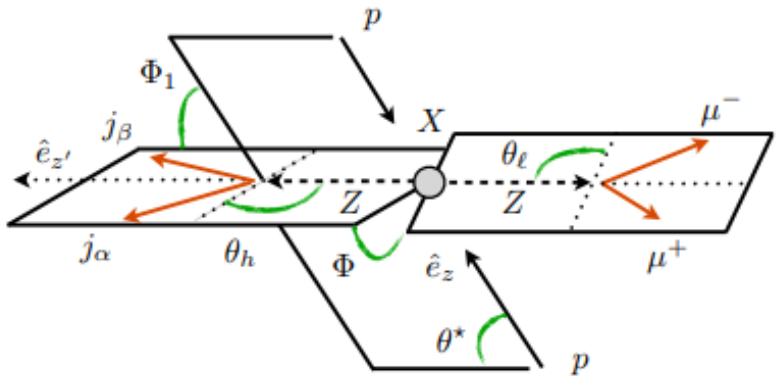


Figure: Angles sensitive to the spin and CP characterization program[26]

[26] arXiv:1010.0676

# Angular Definitions

- $\cos\theta_h$ is the angle between $\vec{p}_\alpha$ (from $Z \to \ell\ell$) and $\vec{p}_X$ (Higgs direction).
- $\cos\theta_l$ is the angle between $\vec{p}_-$ (lepton) and $\vec{p}_X$.
- The Collins-Soper angle ($\cos\theta^*$) is the angle between the beam axis and the $ZZ$ decay axis in the Higgs frame.
- The azimuthal angle $\cos\Phi_1$ correlates the $Z$ decay plane orientation with the beam axis.
- $\cos\Phi$ relates the two $Z$ decay planes.

The expressions are given by:

$$\cos\theta_h = \frac{\tilde{p}_\alpha \cdot \tilde{p}_X}{\tilde{p}_\alpha^2 \tilde{p}_X^2}|_{Z_h}, \quad \cos\theta_l = \frac{\tilde{p}_- \cdot \tilde{p}_X}{\tilde{p}_-^2 \tilde{p}_X^2}|_{Z_l}, \quad \cos\theta^* = \frac{\tilde{p}_{Z_l} \cdot \hat{e}_z}{\tilde{p}_{Z_l}^2}|_X \tag{45}$$

$$\cos\Phi_1 = \frac{(\hat{e}_z \times \hat{e}_z^0) \cdot (\tilde{p}_\alpha \times \tilde{p}_\beta)}{\sqrt{(\tilde{p}_\alpha \times \tilde{p}_\beta)^2}}|_X, \quad \cos\Phi = \frac{(\tilde{p}_\alpha \times \tilde{p}_\beta) \cdot (\tilde{p}_- \times \tilde{p}_+)}{\sqrt{(\tilde{p}_\alpha \times \tilde{p}_\beta)^2 (\tilde{p}_- \times \tilde{p}_+)^2}}|_X \tag{46}$$

Spin-0 Higgs bosons produce specific angular distributions; for example, $\cos\theta^*$ peaks at 0 and $\pi$. Spin-1 and spin-2 bosons yield different distributions.

# CP properties and symmetry transformations

The three discrete symmetries consistent with Lorentz invariance and a Hermitian Hamiltonian are charge conjugation (C), parity (P), and time reversal (T). Their actions are defined as follows:

- **Charge Conjugation (C):** For a scalar field $\phi(t, X)$,

$$C\phi(t, X)C^{-1} = \eta_c \phi^*(t, X) \tag{47}$$

  where $\phi^*$ is the complex conjugate of the scalar field, and $\eta_c$ is a phase factor.

- **Parity (P):**

$$P\phi(t, X)P^{-1} = \eta_p \phi(t, -X) \tag{48}$$

  where $\eta_p$ is the intrinsic parity of the field.

- **Time Reversal (T):**

$$T\phi(t, X)T^{-1} = \phi(-t, X) \tag{49}$$

# Transforming to Momentum-Spin Space

terms of momentum ($\vec{p}$) and spin ($\vec{s}$), the transformations take the form:

$$C : C|\phi(p,s)\rangle = |\phi^*(p,s)\rangle \quad \text{(swaps particle and antiparticle states)}$$
$$P : P|\phi(p,s)\rangle = \eta_p|\phi(-p,s)\rangle \quad \text{(flips momentum, keeps spin)}$$
$$T : T|\phi(p,s)\rangle = \langle\phi(-p,-s)|$$

# Observables and Symmetry Tests

An observable is a measurable quantity like momentum and spin. Observables can be classified based on their behavior under C, P, and T:

- **U-even observable:** $O(U|i\rangle \to U|f\rangle) = +O(|i\rangle \to |f\rangle)$ (remains unchanged).
- **U-odd observable:** $O(U|i\rangle \to U|f\rangle) = -O(|i\rangle \to |f\rangle)$ (changes sign).

If the underlying physics respects U symmetry, the average of a genuine U-odd observable is zero. This helps test symmetry violation.

| Observable | Theory | Re-scattering | Prediction |
|---|---|---|---|
| CP-odd, $\hat{T}$-odd | CP-symmetric | no | $\sigma_{\text{int}}$ symmetric, odd $O \Rightarrow \langle O \rangle = 0$ |
| | | yes | $\sigma_{\text{int}}$ symmetric, odd $O \Rightarrow \langle O \rangle = 0$ |
| | CP-violating | no | Can have $\langle O \rangle \neq 0$ |
| | | yes | Can have $\langle O \rangle \neq 0$ |
| CP-odd, $\hat{T}$-even | CP-symmetric | no | $\sigma_{\text{int}}$ symmetric, odd $O \Rightarrow \langle O \rangle = 0$ |
| | | yes | $\sigma_{\text{int}}$ symmetric, odd $O \Rightarrow \langle O \rangle = 0$ |
| | CP-violating | no | $\sigma_{\text{int}}$ anti-symmetric, even $O \Rightarrow \langle O \rangle = 0$ |
| | | yes | Can have $\langle O \rangle \neq 0$ |

For LHC analysis, CP transformation properties relate to T transformation. If CP is conserved, the expectation value of a T-odd observable is zero, whereas a nonzero value indicates CP violation.

# CP Tests at Hadron Colliders

At the LHC, collisions of quarks and gluons produce particles, but we cannot measure their spins or charges directly. Instead, we analyze their momenta. Scalar products of momenta help define CP observables.
Using the Levi-Civita tensor, we construct a unique P-odd and T-odd observable to test CP violation. Higgs processes define three CP-odd observables: two CP-odd, T-even (from scalar products) and one CP-odd, T-odd (from Levi-Civita construction).

Here are some Feynman diagrams describing three processes useful for analyzing Higgs CP properties: WBF Higgs production, associated Zh production and $h- > 4l$ decays respectively.

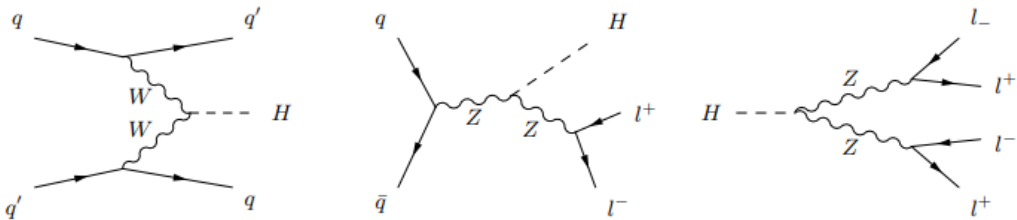


Figure: : Feynman diagrams describing three processes useful for analyzing Higgs CP properties: WBF Higgs production, associated Zh production, and h $\rightarrow$ 4l decays.

# Outline

# Transformer based measurements of ttH

Run-2 measurements of the $ttH(bb)$ process give a twice as much signal significance[27]! Entirely due to better classification schemes, better $b$-jet identification based on artificial neural networks. Better separation from backgrounds too.

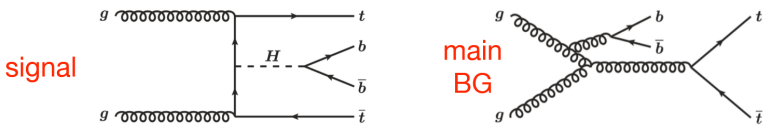


Figure: By Giagu S., ATLAS collaboration, BCVSPIN2024

[27] https://arxiv.org/abs/2407.10904

# ttH measurements

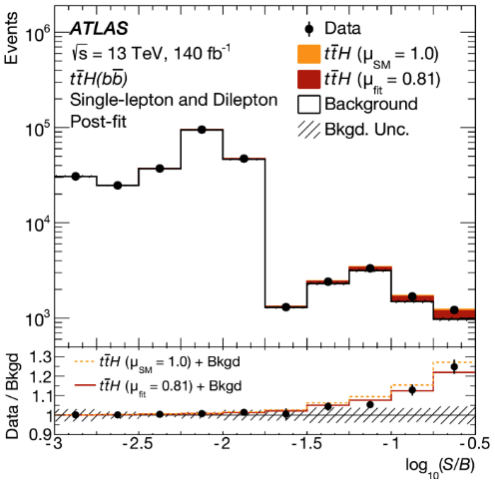


Figure: $ttH$ signal strength, $m_H = 125.09$ GeV is $\mu_{t\bar{t}H} = 0.81 \pm 0.11(\text{ stat.})^{+0.20}_{-0.16}(\text{ sys.})$

# Off-shell Higgs production from $ZZ$ leptonic decays[28]

Uses the following relations:

On-shell

$$\sigma^{\text{on-shell}}_{gg\to H\to ZZ} \sim \frac{g^2_{ggF} g^2_{HZZ}}{m_H \Gamma_H}$$

Off-shell

$$\sigma^{\text{off-shell}}_{gg\to H\to ZZ} \sim \frac{g^2_{ggF} g^2_{HZZ}}{m^2_{ZZ}} \text{ (independent of decay width)}$$

Off-shell production accessible as ZZ decay phase space for the increases, balances out the expected drop in the production at higher masses

[28] Physics Letters B, Volume 846, 2023, 138223

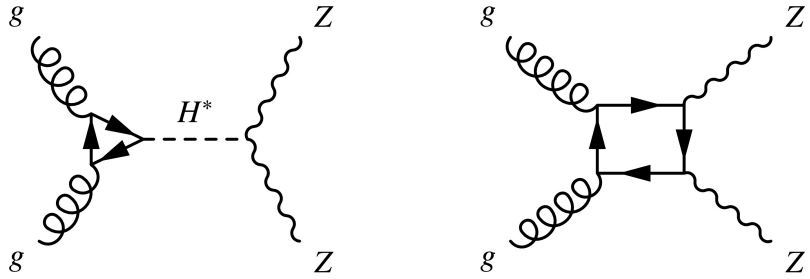


Figure: The leading-order Feynman diagrams for the (a)$gg \to H^* \to ZZ$ signal and (b) background processes

## Neural Simulation-Based Inference (NSBI):

Allows continuous ML-based approximation of full matrix elements at detector level. 20% better sensitivity to off-shell Higgs production.

# Higgs self-coupling constraints[29]

- Self interactions are characterized by the trilinear self-coupling $\lambda_{HHH}$
- In SM: $\lambda_{HHH} = (m^2 G_F)/\sqrt{2}$
- Analysis of $\kappa_\lambda = \lambda_{HHH}/\lambda_{HHH}^{SM}$
- Important as typical Higgs cross sections get modified if the self-coupling deviates from SM predictions.
- Double-Higgs production is directly sensitive to the Higgs boson self-coupling, starting at the lowest order in perturbation theory.
- ggF HH accounts for 90% of production, followed by VBF.

[29] arXiv:2211.01216v2

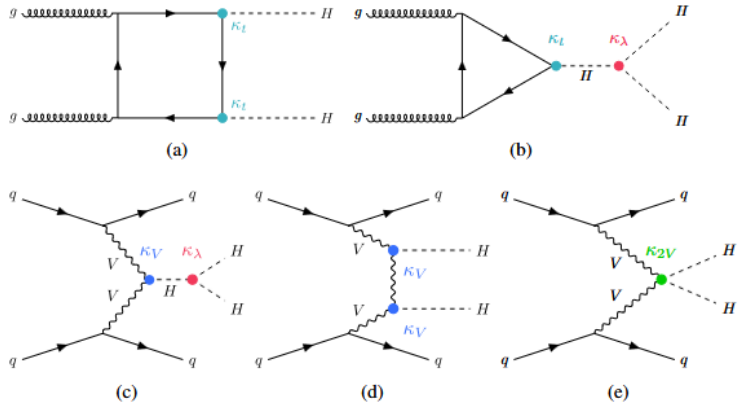


Figure: (a) and (b) are ggF production mechanisms, while (c), (d) and (e) are VBF mechanisms.

# Decay channels involved

| Analysis channel | Integrated luminosity [fb$^{-1}$] |
|---|---|
| $HH \to b\bar{b}\gamma\gamma$ | 139 |
| $HH \to b\bar{b}\tau^+\tau^-$ | 139 |
| $HH \to b\bar{b}b\bar{b}$ | 126 |
| $H \to \gamma\gamma$ | 139 |
| $H \to ZZ^* \to 4\ell$ | 139 |
| $H \to \tau^+\tau^-$ | 139 |
| $H \to WW^* \to e\nu\mu\nu$ (ggF,VBF) | 139 |
| $H \to b\bar{b}$ $(VH)$ | 139 |
| $H \to b\bar{b}$ (VBF) | 126 |
| $H \to b\bar{b}$ $(t\bar{t}H)$ | 139 |

Figure: Single and di-Higgs decay channels included in constraining the self-coupling

# Constraints in the $\kappa_\lambda - \kappa_t$ plane

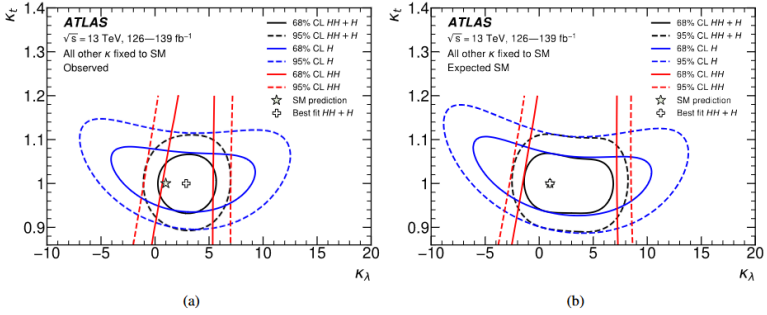


Figure: Observed (a) and expected (b) constraints in $\kappa_\lambda - \kappa_t$ plane from single Higgs (blue), double Higgs (red) analyses and their combination (black)